Hindawi
Wireless Communications and Mobile Computing
Volume 2021, Article ID 8337419, 14 pages
https://doi.org/10.1155/2021/8337419

Research Article

Joint Channel Allocation and Power Control for Uplink NOMA-Assisted Multi-UAV Networks

Shaojie Wen,[1] **Lianbing Deng**,[1] **and Zengliang Liu**[2]

[1]*Zhuhai Da Hengqin Science and Technology Development Co., Ltd., China*
[2]*Institute of Information Operation, National Defence University of PLA, Beijing 100091, China*

Correspondence should be addressed to Lianbing Deng; dhqscience@dhqtech.com

Received 21 July 2021; Revised 15 September 2021; Accepted 13 December 2021; Published 29 December 2021

Academic Editor: Quoc-Tuan Vien

The explosive growth of data leads to that the traditional wireless networks cannot enable various quality of service (QoS) communication for cellular-connected multi-UAV (unmanned aerial vehicle) networks. To overcome this obstacle, we solve the joint optimization problem of channel allocation and power control for uplink NOMA-assisted multi-UAV networks. Firstly, we design a mixed integer nonlinear programming framework, where the channel gains are characterized with integral form in time interval and sorted in nondescending order as the priority index of the decoded signal. In order to propose a feasible algorithm, the initial power levels of UAVs are obtained and integrated into the original problem which is reduced to integer programming problem. Then, the UAVs whose channel gain differences satisfy the constraints will be divided into a group to share the same channel, while the initial power levels of UAVs are adjusted to get a more satisfactory initial solution for power control. Combining the solution of channel allocation and the initial power levels, we solve power control problem with asynchronous update mechanism until the power levels of UAVs remain unchanged. Finally, we propose a channel allocation algorithm and a power control algorithm with the asynchronous optimization mechanism, respectively. Simulation results show that the proposed algorithms can effectively improve the network performance in terms of the aggregated rate.

1. Introduction

Unmanned aerial vehicle (UAV) systems have been widely used in different scenarios because of its flexibility, especially in civilian applications, such as for aerial surveillance, moving target tracking, environment monitoring, and communication relaying [1]. However, most UAV systems controlled by handle manipulator are limited by their simple functions and limited coverage; so, it cannot be extended to more applications. Fortunately, cellular-connected UAV [2] can break restrictions faced by traditional UAV systems, where UAVs are integrated into the cellular networks as new aerial users. In addition, the explosive growth of data collected by UAVs increases the complexity of application environment. Therefore, the traditional cellular technique (e.g., 3G/4G) cannot provide real-time communication services. As a promising candidate for 5G communications [3], Non-Orthogonal Multiple Access (NOMA) [4] can provide higher spectral efficiency, ultra reliable/low latency communication, and network throughput compared to Orthogonal Multiple Access (OMA) technique. As a consequence, applying NOMA technique to cellular-connected UAV networks can effectively improve the channel capacity and ensure the timeliness of the data transmission.

In the multichannel uplink NOMA-assisted communication, the system needs to allocate the corresponding channel resources for each terminal equipment and decrease the interference level between signals by controlling the power level of the terminal equipments to maximize the network throughput. However, the high mobility of UAV causes the channel state to change rapidly between UAV and ground base (GB) [5], which increases the complexity to design the channel allocation and power control algorithm. Although the traditional channel allocation and power control methods for cellular networks [6] meet the requirements of the small-scale data transmission, these proposed methods would enconuter poor performances in terms of bandwidth resources with the increasing number of UAVs. An alternative is to integrate

power-domain NOMA technique into cellular network [7], which allows the terminal equipments to transmit signals concurrently on the same channel with the channel gain differences. The successive interference cancellation (SIC) technology is used to decode superimposed signals at GB to improve bandwidth utilization and effective network throughput. Therefore, it is of great significance to study the channel allocation and power control algorithm in NOMA-assisted multi-UAV network.

This work is aimed at maximizing the channel capacity by allocating the channel resources and controlling the power levels of UAVs. Because the channel capacity is a nonlinear function with the power as parameter, hence we design a mixed integer nonlinear programming framework to mathematically represent the channel allocation and power control problem and propose a distributed algorithm to meet the QoS requirements. Firstly, we get the initial power levels of the UAVs when the channel capacity constraint holds. The initial power levels of the UAVs are integrated into the original problem which is reduced to integer programming problem (namely channel allocation problem). Then, the average channel gains are sorted in nondescending order as the priority index of the decoded signal at GB. Next, we divide the UAVs whose channel gain differences satisfy the constraints into a group, in which the group number should be no more than the upper bound served by each channel. When each UAV is associated with a specific channel, we adjust the power levels of UAVs with asynchronous update [8] mechanism until the power levels of UAVs remain unchanged. Finally, we propose a channel allocation algorithm and a power control algorithm, which consider the effects of UAVs' fast mobility and the initialization parameters on the optimization performance. Our contributions are twofold as follows:

(i) We design a mixed integer nonlinear programming framework as the mathematical form for the uplink channel allocation and power control problem. To enable the corresponding optimization process to be applied in the dynamic scenario, the channel gain is characterized with integral form instead of the instantaneous form and sorted in nondescending order as the priority index of the decoded signal at GB. As the joint optimization problem is difficult to solve, a distributed method with low computational and time complexity is proposed. To this end, we calculate the initial power levels of UAVs and integrate them into the original problem to get the solution of integer programming. Then, we combine the asynchronous update mechanism and successive convex approximation to obtain the optimal power levels of UAVs

(ii) We propose a channel allocation algorithm and a power control algorithm with asynchronous optimization mechanism. In the channel allocation process, the initial power levels of UAVs are adjusted after each UAV is assigned to a specific channel, which enables the initial solution for the power control issue to meet the requirements of the different constraints in the feasible region. The asynchronous optimization method considered in power control algorithm allows GB to update the distinct power parameters with outdated messages, which can well adapt to the unreliability of the wireless communication

The remainder of this paper is organized as follows. In Section 2, we introduce some previous work. In Section 3, we present some preliminary concepts used in the proposed method. In Section 4, we introduce the specific implementation process of the proposed channel allocation and power control algorithm. And in Section 5, we show some simulation results for the proposed algorithm. Finally, we conclude the paper and discuss future work in Section 6.

2. Related Work

As one of the key techniques of 5G, NOMA has been studied a lot [9] and gradually applied in real world. In addition, the combination of NOMA with other emerging technologies (such as massive MIMO and visible light communications) also has been considered to further increase scalability, spectral efficiency, reliability, and greenness of future communication networks [10]. The existing works have mainly studied the performances of downlink and uplink in 5G and beyond 5G networks from different views and scenarios, such as channel knowledge [11], boadcast/unicast convergence [12], and full-duplex heterogeneous networks [13].

Some research have studied the related issues on uplink communication, and Liu et al. [14] developed an analytical framework for multicell uplink NOMA systems based on stochastic geometry and derived the Laplace transform of the intercell interference with considering uplink power control. Zeng et al. [15] studied an energy efficiency maximization problem by jointly optimizing the user clustering, channel assignment, and power allocation for an uplink hybrid system with the integration of NOMA and OMA. Chen et al. [16] developed user selection and power allocation methods for NOMA systems equipped with multiantenna to enhance the sum capacity of the uplink. And they derived a user set selection algorithm and a suboptimal power control algorithm to mitigate the interference effect and to maximize the sum capacity. Jointly considering the heavy computation workload raised by the sizable networking systems and the difficulty in estimating instantaneous Channel State Information (CSI), Zhao et al. [17] solved a joint power control and channel allocation problems based on reinforcement learning algorithm combining with statistical CSI. Rashid et al. [18] investigated MC-NOMA technology for enhancing system energy efficiency (EE) by formulating a joint user clustering, subchannel allocation, and power allocation problem for EE maximization in uplink MC-NOMA scenario. To solve the optimization problem of the user grouping, decoding order and power control in an uplink NOMA system, Zhang et al. [19] formulated a joint optimization problem as combinatorial integer programming framework to maximize the achievable sum rate of the multiple users with the minimum rate

requirement. Zamani et al. [20] investigated weighted sum EE in uplink and downlink of a multiuser NOMA system and formulated the signal processing power as a linear function of transmit power.

Applying NOMA technique to UAV-enabled communication has become a research hotspot, where UAVs are used as flying base stations to provide ubiquitous connections for mobile devices in over-crowded areas. Lu et al. [21] investigated the UAV enabled uplink NOMA network to overcome the inherent latency in multi-UAV networks with orthogonal multiple access. They jointly optimized the UAV deployment position and the power control to maximize the sum rate of all users and to meet the QoS requirement. Because the secure transmission of NOMA-UAV networks remains a great challenge, Chen et al. [22] summarized several potential solutions to mitigate adversarial eavesdropping toward aerial-ground transmission and propose three effective security schemes. To overcome the combinatorial nature and nonconvexity of the joint placement design, admission control, and power allocation in NOMA-based UAV systems, Tang et al. [23] proposed a low complexity mechanism based on the penalty function method and the successive convex approximation to maximize the number of users with satisfied QoS experience.

The studies in [21–23] mainly use the UAV as the flying base stations; however, some researches take UAVs as aerial users to design communication architecture in cellular-enabled networks. Zhang et al. [24] considered two main research paradigms in cellular-enabled UAV communication and UAV-assisted cellular communication. The former regarded UAVs as new aerial users served by GB, and the later took UAVs as new aerial communication platforms serving the terrestrial users. To maximize the sum rate of uplink from UAV to BSs in a specific band, Pang et al. [25] investigated the uplink transmission in a cellular network from a UAV and ground users to base stations via optimizing the precoding vectors. Senadhira et al. [26] studied an emerging cellular-connected UAV architecture for surveillance or monitoring applications, where a cellular-connected aerial user equipment moves along a given trajectory and uses a given data rate to transmit messages in uplink periodically. New et al. [27] considered a downlink wireless communication system with the coexistence of ground user (GU) and mobile aerial user (AU) and investigated the maximum achievable GU rate that satisfied the AU QoS requirement with perfect and partial CSI.

The solutions presented above do not consider both the changes in channel states and the impact of the constant initial power levels on the power control issue. In addition, the existing NOMA-based access schemes are mostly used in cellular networks and rarely applied to multi-UAV networks; hence, the presented solutions cannot be used directly for the joint channel allocation and power control problem in NOMA-assisted multi-UAV networks. Different from previous ideas, in order to adapt the proposed method to the dynamic channel states better, the channel gain in our work is characterized with average form instead of instantaneous form. And the initial power levels of UAVs are adjusted while the channel allocation algorithm is implemented, which aims to get the feasible solution for the power control issue.

3. System Model

3.1. Network Model. The network mainly consists of a single GB that serves as the destination of data flows and multiple UAVs which are independently and uniformly distributed in the deployed area. Assume that the coordination of GB is unchangeable, all the UAVs communicate with GB in single-hop mode, as shown in Figure 1. In this paper, we focus on the uplink data transmission, where the bandwidth W at GB is divided into the orthogonal channels. UAVs transmit the messages to GB via a single channel at any time, and NOMA technique allows the superposed signals from multiple UAVs to be transmitted simultaneously through the same channel. Assume that UAVm and UAV$m+1$ are assigned to the same channel, these two UAVs are allowed to send signals (e.g., temperature, humidity, and wind speed) simultaneously to GB with the uplink from UAVs to GB. To avoid the channel overloading, the maximum number of UAVs that each channel can serve should be no more than K. We use C to denote a set including all channels, and $|C|$ and c_n denote the identifier of nth channel and the number of the channels, respectively. The set of UAVs is denoted by the notation M, the size of M is M, and the set of UAVs assigned to channel c_n is denoted as M_n. The power level p_m used by UAVm is limited in the range $[p_{\min}, p_{\max}]$. The definitions of notations or parameters can be found in Table 1.

3.2. Channel Model. Due to the mobility, the distance between UAVs and GB changes with time elapse which results in the variable channel states. Fortunately, the channel state prediction method proposed in [28] can capture this dynamic nature and estimate the channel gain value for each UAV after Δt time. Assume that the current time is t_0, the future time is t after Δt. The quantity $h(t \mid t_0)$ represents the channel gain prediction at t based on the information available at t_0; hence, it is a random variable due to the uncertainty in mobility over the time duration from t_0 to t. If $t_0 = t$, the quantity $h(t \mid t_0)$ is equal to the instantaneous channel gain value [29] at t.

Assume that all the UAVs follow the same mobility model, let $f_y(y)$ (the detailed form refers to the expressions (20)-(21) in the reference [29]) represents the probability density function of distance y at current time, and $g(y)$ (the detailed form can refer to the Rican model [30]) denotes the path fading gain of links between UAVs and GB. Let $y(t_0)$ denote a function of distance between UAVs and GB at t_0; so, the expected channel gain for each UAV can be expressed as an integral form

$$\mathbb{E}[h(t \mid t_0)] = \int_{t_0}^{t} g(y(t)) \cdot f_y(y(t)) \mathrm{d}t. \tag{1}$$

Expression (1) quotes the definition (24) in reference [29], and the slight difference lies in the different objects of integration. The expected channel gain in (1) can reflect

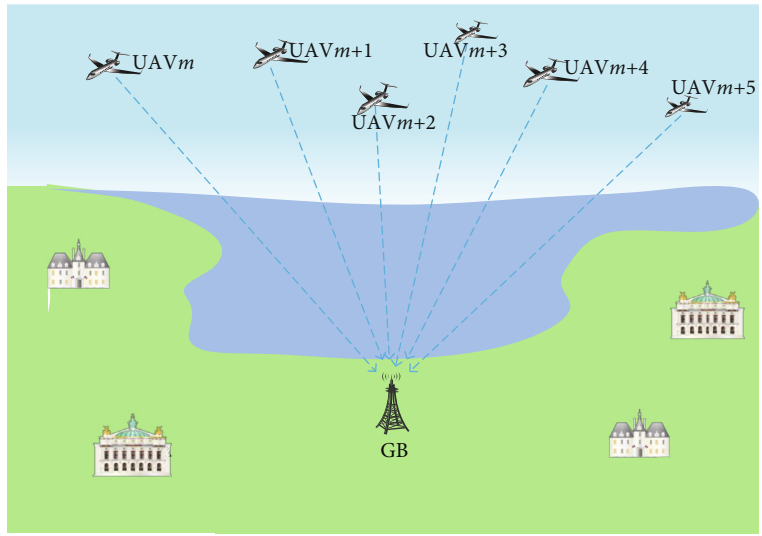

Figure 1: Multi-UAV network model.

Table 1: Simulation parameters.

Parameter	Value
Area size	1000 m × 1000 m × 80 m
The number of UAVs	[10, 50]
Transmission radius	1000 m
The number of subchannels	10
Maximum power level	1 W
Noise	-36 dBm
Mobility model	Random way point
Channel model	Rican model
Bandwidth W	5 MHz
Subchannel size	0.5 MHz
Transmission rate threshold	[0.1 Mbps, 0.7 Mbps]
Path loss coefficient	2.65

the link quality well; however, the fast changing channel state would result in the outdated message used by GB in a specific duration $[t_0, t]$. The channel gain calculated by (1) only reflect the channel states at a destined point in the future, and it is necessary to find a way which can reflect the channel states in the duration $[t_0, t]$ accurately and assist the GB to optimize the network performance. Hence, the average channel gain denoted by $\bar{h}$ is introduced to represent the link quality in time interval Δt, and the mathematical expression is listed as below.

$$\bar{h} = \frac{1}{\Delta t} \sum_{x=t_0}^{t} \int_{t_0}^{x} g(y(t)) \cdot f_y(y(t)) \mathrm{d}t, \tag{2}$$

where x is a transition variable. The use of NOMA technique depends on the channel gain differences between UAVs, better communication performance for the whole network benefits from larger channel gain differences. Therefore, we divide UAVs with larger channel gain differences into a group to share the same spectrum resource. Before that, we need to get the nonascending order of the UAVs' channel gains, namely, $\bar{h}_1 \geq \bar{h}_2 \cdots \geq \bar{h}_M$, where the subscripts are regarded as the identifier of UAVs.

4. Problem Formulation and Solution

4.1. Problem Formulation. This work mainly focuses on the channel allocation and power control for NOMA-assisted multi-UAVs networks. In order to identify which channel a single UAV is assigned to, a binary variable is defined as a_m^n, where the superscript n and subscript m indicate the channel c_n and mth UAV, respectively. If the mth UAV is assigned to the channel c_n, then $a_m^n = 1$; otherwise, $a_m^n = 0$.

$$a_m^n = \begin{cases} 1, & \text{if UAV } m \text{ is assigned to the channel } c_n. \\ 0, & \text{otherwise.} \end{cases} \tag{3}$$

Because the NOMA technique decodes the massages according to the strength of the signal, the weaker signals will be considered as interference of the priority decoded signals in the same channel M_n. Assume that the signal from UAVm currently is decoded, the sum of the weaker signals from the other UAVs in M_n is the interference of UAVm, namely, $\sum_{\substack{i \in M_n \\ \bar{h}_i \leq \bar{h}_m}} a_i^n p_i \bar{h}_i^2$. To evaluate the network performance more intuitively, we optimize the channel capacity of each UAV, and which is given as below:

$$R_m = \log \left(1 + \frac{p_m \bar{h}_m^2}{\sum_{\substack{i \in M_n \\ \bar{h}_i \leq \bar{h}_m}} a_i^n p_i \bar{h}_i^2 + \sigma^2} \right), \tag{4}$$

where σ^2 is the additive white Gaussian noise. For the ease of

expression, we define a normalized channel gain for the mth UAV as $g_m = \bar{h}_m^2/\sigma^2$; so, the formula (4) can be rewritten as

$$R_m = \log\left(1 + \frac{p_m g_m}{\sum_{\substack{i \in M_n \\ \bar{h}_i \le \bar{h}_m}} a_i^n p_i g_i + 1}\right). \tag{5}$$

The capacity of the last component decoded on the channel c_n is $R_f = \log(1 + p_f g_f)$.

Based on the binary variable and link capacity calculated in (5), we define the problem in a mathematical form with aggregated channel capacity of UAVs as the objective function, the detailed form is expressed as follows:

$$\max \sum_{n \in C} \sum_{m=1}^{M} a_m^n R_m, \tag{6}$$

$$s.t. R_m \ge R_m^{th}, \forall m \in M, \tag{7}$$

$$p_m g_m - \sum_{n \in C} \sum_{\substack{i \in M \\ \bar{h}_i \le \bar{h}_m}} a_i^n p_i g_i \ge p_{th}, \forall m \in M, \tag{8}$$

$$p_{\min} \le p_m \le p_{\max}, \forall m \in M, \tag{9}$$

$$\sum_{m=1}^{M} a_m^n \le 1, \forall n \in C, \tag{10}$$

$$\sum_{n \in C} a_m^n \le K, \forall m \in M, \tag{11}$$

$$a_m^n \in \{0, 1\}, \forall m \in M, \forall n \in C. \tag{12}$$

Optimization objective (6) maximizes the sum of all UAVs' channel capacity. Constraint (7) ensures that the channel capacity used by the UAVs is no smaller than the given threshold to meet the requirement of correct decoding. Constraint (8) represents SIC requirement for correct decoding of superimposed signals at GB, and (9) limits the maximum power levels of UAVs. Constraint (10) means that any UAV can only transmit signals on one channel at a specific time. On the premise of ensuring the decoding rate, (11) limits the number of concurrent signals in a single channel.

$M \le |C|$, namely, the number of channels, is not less than the number of UAVs, such that each UAV can occupy a channel independently due to the orthogonality between different channels. In this situation, a single UAV selects the maximum power level to transmit signals to improve network performance. We mainly discuss how to allocate channels and adjust power level to maximize network throughput when $2 | C | \le M \le K|C|$. The optimization problem defined in (6)–(12) is a mixed integer nonlinear programming (MINLP) problem [31], which has been proved to be *NP*-hard. Therefore, it is necessary to find a distributed solution which not only achieves the optimization goals for joint channel allocation and power control issues, but also maximizes the network throughput.

4.2. Distributed Solution. Because it is difficult to get the optimal solution of MINLP problem defined above, so an approximate solution is necessary for the improvement of communication performances. The best effect of optimization is to make the final solution as close to the optimality as possible; hence, the initial feasible parameters are important to get the optimal solution. On this basis, we calculate the initial power levels of UAVs by only considering the environmental noise σ^2 when the equality relation of the constraint (7) holds, namely,

$$\log\left(1 + p_m^{ini} g_{\mathrm{m}}\right) = R_m^{th}, \forall m \in M. \tag{13}$$

The initial feasible power level of the mth UAVs can be obtained by mathematical calculation,

$$p_m^{ini} = \frac{2^{R_m^{th}} - 1}{g_m}, \forall m \in M, \tag{14}$$

and we set the initial power level of each UAV to $p_{\max}^{ini}$, where $p_{\min} \le p_{\max}^{ini} \le p_{\max}$ and $p_{\max}^{ini} = \max\{p_m^{ini} | \forall m \in \mathrm{M}\}$.

4.2.1. Channel Allocation. To this end, we use the power level $p_{\max}^{ini}$ and equation (5) to obtain the initial rate $R_m^{ini} = \log(1 + p_{\max}^{ini} g_m)$ which is substituted into the optimization problem (6)–(12) to get an integer programming form (channel allocation) P1 as below:

$$\begin{aligned} P1 &: \max \sum_{n \in C} \sum_{m=1}^{M} a_m^n R_m^{\mathrm{ini}}, \\ &s.t. (7), (79) - (7911). \end{aligned} \tag{15}$$

Based on the number of channels $|C|$, the maximum number of UAVs assigned to the same channel can be calculated as $\lceil M/|C| \rceil \le K$, let $U = \lceil M/|C| \rceil$. A cluster set is defined by $M = \{M_1, \cdots, M_n, \cdots, M_N\}$, and all components in M are empty in initialization phase. Next, UAVs are divided into U subsets based on the order of channel gains, $\underbrace{[UAV_1, \cdots, UAV_{|C|}][UAV_{|C|+1}, \cdots, UAV_{2|C|}]}_{S_1 \quad S_2} \cdots \underbrace{[UAV_{M-|C|+1}, \cdots, UAV_M]}_{S_U}$, and each subset S_n consists of at least $|C|$ components. According to the feature of NOMA technique, the later decoded signals will interfere with the previous decoded signals. Therefore, we choose one component from each subset in reverse order and group these components into one cluster to share the same channel. The detailed process is as follows, the component $UAV_{M-|C|+1}$ extracted from set S_U is added to subset M_1, and we choose the component of the corresponding sequence from the subsequent subset, such as $UAV_{|C|+1}$ in set S_2. Before continuing this process, it needs to judge whether the constraint (8) holds, if not, adjust the power level of corresponding UAV to meet the condition. After determining the component in S_1, it ends the current grouping process, and the components included in subset M_1 is denoted as $[UAV_1,$

$UAV_{|C|+1}\cdots,UAV_{M-|C|+1}]$. When all the subsets in M are empty, the channel allocation algorithm is terminated. The detailed implementation process of channel allocation is presented in algorithm 1.

Algorithm 1 shows two advantages when compared with other similar works on channel allocation. One is that Algorithm 1 characterizes the channel gain with average form in interval Δt (Step 4.2.1 in Algorithm 1), which can well adapt to the mobility without declining the communication performance. Other works (such as [32]) consider only instantaneous channel gain. The other advantage is that we adjust the initial power levels of UAVs (Step 4.2.1 in Algorithm 1) to get a more satisfactory initial solution for power control while the channel allocation algorithm is implemented. The main purpose is to make the initial solution for power control satisfy different constraints in the feasible region.

4.2.2. Power Control. The results obtained from Algorithm 1 are substituted to optimization (6)–(12), and a mathematical form of power control problem can be expressed as below:

$$\begin{aligned} &\max \sum_{m=1}^{M} R_m, \\ &s.t. \quad (6), (68), \\ &p_m g_m - \sum_{\substack{i\in M_n \\ \bar{h}_i \le \bar{h}_m}} p_i g_i \ge p_{th}, \forall m \in M_n, \forall M_n \in M. \end{aligned} \tag{16}$$

Due to the orthogonality between different channels, there is no loss of optimality to consider only one single channel for power allocation, and the others use the same method to achieve the goal of power control. Therefore, we choose a channel c_n including K UAVs as a typical optimization object and use a new sequence number $1, \cdots, K$ to replace the original marks of all the UAVs in subset M_n. Hence, the power control problem can be redefined as

$$P2 : \max \sum_{k\in M_n} R_k, \tag{17}$$

$$s.t.(6), (68), \tag{18}$$

$$p_k g_k - \sum_{\substack{i\in M_n \\ \bar{h}_i \le \bar{h}_k}} p_i g_i \ge p_{th}, \forall k \in M_n. \tag{19}$$

The scale of $P2$ is smaller compared with original problem, and the former is easier to get the optimal power levels for all the UAVs in subset M_n. However, the nonconvexity of the capacity function (4) combined with constraints (7), (9), and (19) increases the complexity of obtaining the optimal power levels. To overcome this obstacle, we use successive convex approximation techniques [33] to convert function (5) into a convex form:

$$R_k \approx \alpha_k \left[\log\left(p_k g_k\right) - \log\left(1 + \sum_{i\in M_n} p_i g_i\right) \right] + \beta_k, \tag{20}$$

where α_k and β_k are assistant variables, the detailed forms of which can be found in [34].

Assume that the power levels of UAVs are located in convex domain, hence P2 is a convex optimization problem due to the linearity of constraints. To this end, we introduce three dual vectors to assist the optimization process, denoted by γ, ξ, and ζ, respectively. The dual form of $P2$ can be presented as follows:

$$\begin{aligned} L(p,\gamma,\xi,\zeta) = \max &\sum_{k\in M_n} R_k + \sum_{k\in M_n} \left[\gamma_k \left(p_k g_k - \left(2^{R_m^{th}} - 1\right) \left(1 + \sum_{i\in M_n} p_i g_i\right) \right) \right] \\ &+ \sum_{k\in M_n} \xi_k \left(p_k g_k - \sum_{i\in M_n} p_i g_i - p_{th} \right) + \sum_{k\in M_n} \zeta_k (p_{\max} - p_k). \end{aligned} \tag{21}$$

Although the average channel gain can effectively improve the communication performance, the unpredictable wireless environment will cause that a part of request packets cannot be decoded correctly at GB. Fortunately, the asynchronous optimization can be considered as an alternative solution to solve the above problem. In order to update the parameters asynchronously, we define the notation n as the number of iterations and τ_i^n as the index of the Lagrange multiplier used in the ith minimization and $1 < \tau_i^n < n$. Consider asynchronous optimization, the update process of three dual vectors can expressed as

$$\gamma_k(t+1) = \left[\gamma_k(t) - \beta_1 \frac{\partial L(\tau_i^n)}{\partial \gamma_k} \right]^+, \tag{22}$$

$$\xi_k(t+1) = \left[\xi_k(t) - \beta_2 \frac{\partial L(\tau_i^n)}{\partial \xi_k} \right]^+, \tag{23}$$

$$\zeta_k(t+1) = \left[\zeta_k(t) - \beta_3 \frac{\partial L(\tau_i^n)}{\partial \zeta_k} \right]^+, \tag{24}$$

where $[\cdot]^+$ denotes the projection onto the nonnegative quadrant, and β_1, β_2, and β_3 are step size. In addition, the values of β_1, β_2, and β_3 are constants to speed the convergence of the update process. Jointly consider (22), (23), (24), and one-order derivative of power level p_k, let $\partial L(p, \boldsymbol{\gamma}(t+1), \boldsymbol{\xi}(t+1), \boldsymbol{\zeta}(t+1))/\partial P_k = 0$, we can obtain the optimal power level of each UAV in subset M_n at iteration $t+1$, and this process is terminated until the dual vectors no longer change. The detailed process can be found in Algorithm 2.

4.3. Algorithm Analysis. Assume that the notation T denotes the maximum iterations which can meet the requirement of step 8 in the Algorithm 2, we can get the following conclusion.

Proposition 1. *If $T \le M$, the total time complexity of two algorithm is $O(M^2)$; otherwise, $O(MT)$.*

1://initialization: each UAV sends a request packet (coordination, speed, channel state, etc.) to GB, $n=|C|$;
2: Get the nonascending order of channel gains, $\bar{h}_1 \geq \bar{h}_2 \cdots \geq \bar{h}_M$;
3: Mark the UAV with channel gain $\bar{h}_m$ as m;
4: Obtain the sets $\{S_1, S_2, \cdots, S_U\}$;
5: for each subset M_n, do
6: for $i=U$; $i \geq 1$; i—do
7: if the set S_i is not empty, then
8: Add the nth component in set S_i to subset M_n;
9: Judge whether the components in subset M_n meet constraint (8);
10: If not, adjust the power level of corresponding component in S_i;
11: end if
12: end for
13: $n=n$-1;
14: end for
15: If all UAVs are assigned to the special channels, the algorithm is terminated;
16: return M.

Algorithm 1: Channel allocation algorithm.

1: GB uses the results of channel allocation calculated by algorithm 1 and the optimized initial power levels;
2: Initialize the dual vector $\gamma(0), \xi(0), \zeta(0)$;
3: for each channel c_n of GB do
4: Use (20) to obtain the capacity expression R_k;
5: Calculate optimal power level based on three dual vectors and one order derivative;
6: Use (22), (23), and (24) to update dual vectors;
7: Return to step 5;
8: The algorithm will be terminated until the dual vectors no longer change.
9: end for

Algorithm 2: Power control.

Proof. To obtain the total time complexity of the proposed two algorithms, assume that the cost for exchanging the beacon information among any a pair of nodes is $O(1)$, we first analyze the time complexity of Algorithm 1; in initialization phase, each UAV exchanges the beacon information with GB, and the time complexity can be denoted as $O(M)$. The step 2 is the sorting process, and the time complexity of this operation is equal to the time complexity of the sorting algorithm in the worst case $O(M^2)$. Steps 5-11 are the sequential grouping process and the adjustment operations of the power levels, and the total time complexity is $O(M)$; hence, the total time complexity of Algorithm 1 is $O(M^2)$. For Algorithm 2, the time complexity of the initial process is $O(3M)$. The steps 3-7 aim to get the optimal power levels, and the time complexity is $O(MT)$. To conclude the above results, if $T \leq M$, the total time complexity of two Algorithm is $O(M^2)$; otherwise, $O(MT)$.□ □

To analyze the proposed algorithms, we provide some auxiliary parameters to illustrate the presented results. Let $g(p_k) = \{(2^{R_m^{th}} - 1)(1 + \sum_{i \in M_n} p_i g_i) - p_k g_k, \sum_{i \in M_n} p_i g_i + p_{th} - p_k g_k, p_k - p_{\max}\}$ denote a set including different constraints and $\|\cdot\|$ be Euclidean norm. We use a constant stepsize β instead of β_1, β_2, and β_3. Two vector notations χ and φ are used to denote the primal variable set and dual variable set, respectively, $\chi = \{p_k | \forall k \in M\}$ and $\varphi = \{\gamma, \xi, \zeta\}$. To simplify the symbolic representations, the joint optimization problem P can be rewritten in a more general form,

$$P: \max F(\chi), \quad s.t. g(\chi) \leq 0. \tag{25}$$

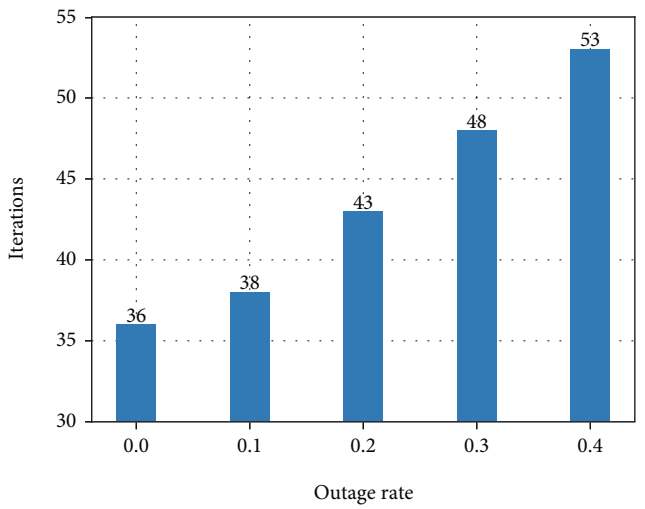

Figure 2: The iterations of each subchannel with two users under different outage rates.

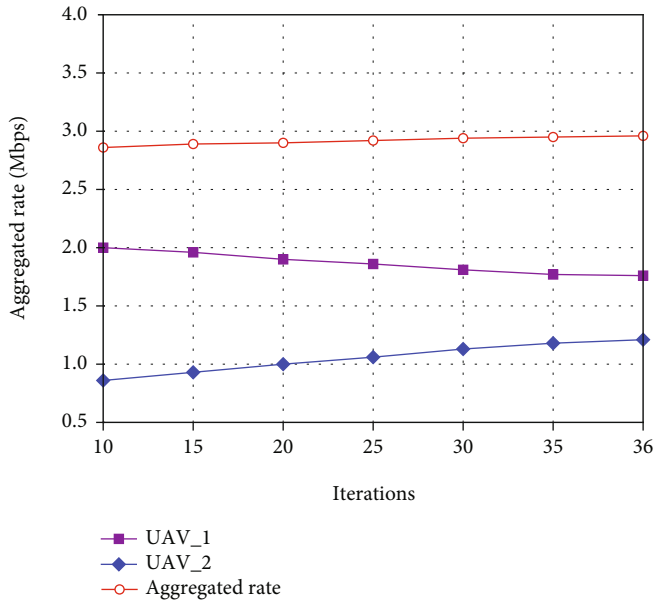

Figure 3: The aggregated rate of each subchannel with two users and the trend of transmission rate of both users under different iterations.

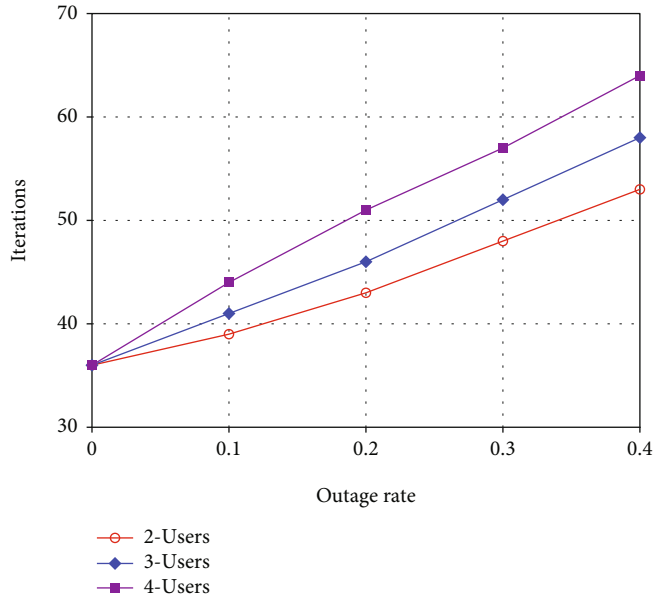

Figure 4: The iterations of single subchannel with different users under different outage rates.

Therefore, the dual iterations (22)-(24) can be rewritten in the following form:

$$\varphi(n+1) = [\varphi(n) + \beta \cdot g(\chi(\tau_i^n))]^+. \tag{26}$$

Assume that the dual form of P is denoted as $D(\varphi)$, the following two conditions are adopted for problem P and iterations (22)–(24).

C1. Set Ψ is convex, closed, and bounded. Combined objective function of problem P and constraint set $g(\chi)$ are convex and continuous over their domain. Assume that there is one set $\{\chi \in \Psi\}$ that makes (7), (8), and (9) hold as strict inequalities.

C2. There exists an integer $D_{\max}$, so that $n - \tau_i^n \le D_{\max}$ and $n = 1, 2, \cdots$.

The first condition asserts the boundedness of the subgradients, and there is a finite bound set $G_{\max}$ that for all $\chi \in \Psi$ the following inequality holds:

$$\|g(\chi)\| \le G_{\max}. \tag{27}$$

Proposition 2. *According to condition C1 and the strict convexity of the optimization problem P2 considering equation*

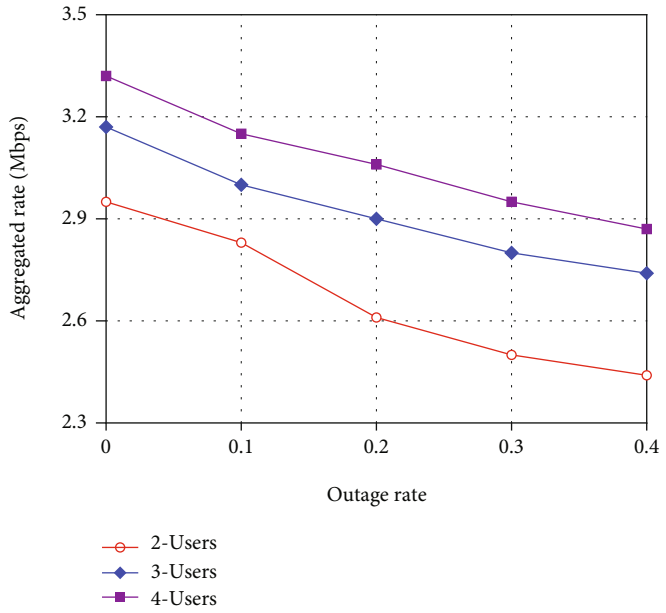

Figure 5: The aggregated rate of single subchannel with different users under different outage rates.

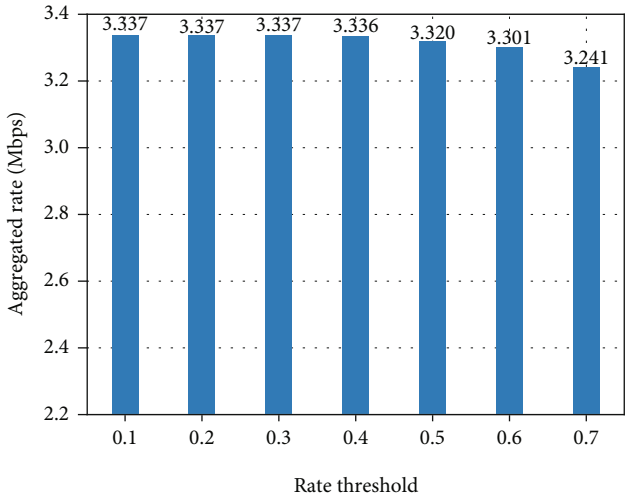

Figure 6: The aggregated rate of single subchannel with four users under different transmission rate thresholds $R_m^{th.}$

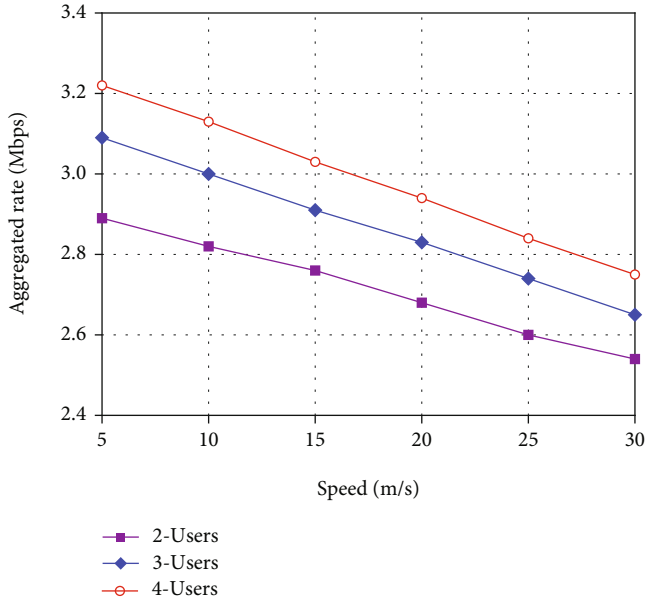

Figure 7: The aggregated rate of single subchannel with different users under different speeds.

(20), it is noted that if the Slater's condition holds, then the duality gap is exactly zero, i.e., $P(\chi^*) = D(\varphi^*)$.

The second condition states that the delay $n - \tau_i^n$ is upper bounded by a finite number. Note that $D_{\max} = 0$ yields the corresponding results for the synchronous algorithm.

We use the pertinent definitions considered in [35] to obtain the following result. Under the condition C1, it holds for all $\varepsilon \geq 0$ and $n = 1, 2, \cdots$ that

$$g(\chi(\tau_i^n))(\varepsilon - \varphi(n)) \leq D(\varepsilon) - D(\varphi(n)) + o(n), \tag{28}$$

where $o(n) = 2\beta \cdot G_{\max}^2 D_{\max}$. The interested readers can refer to the detailed Proof in [35]. Moreover, we propose the following proposition to deal with convergence of Lagrange multiplier that iterates with different stepsizes.

Proposition 3. *Under C1 and C2, the average dual solution* $D(\varphi)$ *and the optimal dual solution* $P(\chi^*)$ *satisfy the following relation:*

$$D(\varphi) \leq P(\chi^*) + \frac{1}{2}\beta G_{\max} + 2\beta G_{\max}^2 D_{\max}. \tag{29}$$

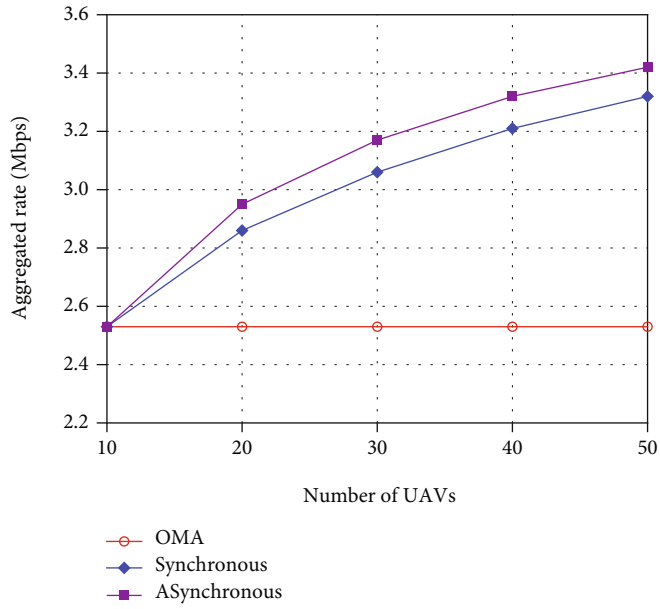

Figure 8: The aggregated rate under different number of UAVs, where each subchannel is assigned two UAVs.

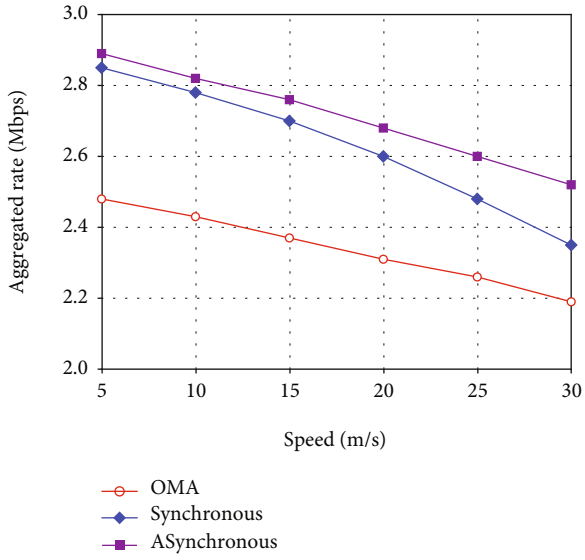

Figure 9: The aggregated rate under different speeds, where each subchannel is assigned two UAVs.

Proof. Let φ^* denote the optimal solution of D. We have the form for all $\varepsilon \geq 0$:

$$\|\varphi(n+1)-\varepsilon\|^2 = \left\|\left[\varphi(n)+\beta g(\chi(\tau_i^n))\right]^+ - \varepsilon\right\|^2. \tag{30}$$

Due to the nonexpansive property of the projection, (30) satisfies the following relation

$$\begin{aligned}\|\varphi(n+1)-\varepsilon\|^2 &\leq \|\varphi(n)+\beta g(\chi(\tau_i^n))-\varepsilon\|^2 \\ &\leq \|\varphi(n)-\varepsilon\|^2 + \|\beta g(\chi(\tau_i^n))\|^2 \\ &\quad + 2\beta g(\chi(\tau_i^n))(\varphi(n)-\varepsilon).\end{aligned} \tag{31}$$

Introducing (27) and (28) into (31), we can get a new form

$$\begin{aligned}\|\varphi(n+1)-\varepsilon\|^2 \leq \|\varphi(n)-\varepsilon\|^2 &+ \beta^2 G_{\max}^2 \\ &+ 2\beta[D(\varepsilon)-D(\varphi(n))] + 4\beta^2 G_{\max}^2 D_{\max}.\end{aligned} \tag{32}$$

Summing the later for $n = 1, 2, \cdots, N$, it follows that

$$\begin{aligned}\|\varphi(n+1)-\varepsilon\|^2 \leq \|\varphi(1)-\varepsilon\|^2 &+ N\beta^2 G_{\max}^2 \\ &+ 2\beta\left[ND(\varepsilon) - \sum_{n=1}^{N} D(\varphi(n))\right] \\ &+ 4\beta^2 G_{\max}^2 D_{\max}.\end{aligned} \tag{33}$$

Let the left-hand side of (33) be 0, rearrange the inequality, and divide it by $2N\beta$, we obtain

$$\begin{aligned}\frac{1}{N}\sum_{n=1}^{N} D(\varphi(n)) \leq \frac{\|\varphi(1)-\varepsilon\|^2}{2N\beta} &+ \frac{1}{2}\beta G_{\max}^2 \\ &+ D(\varepsilon) + 2\beta G_{\max}^2 D_{\max}.\end{aligned} \tag{34}$$

□ □

Let $\varepsilon = \varphi^*$ and $1/N\sum_{n=1}^{N} D(\varphi(n)) = D(\varphi(n))$. We have $\min_{N\longrightarrow\infty}\varphi(1) - \varphi^*/2N\beta \longrightarrow 0$ due to the infinite value of φ^*. Thus, taking the limit as $N \longrightarrow \infty$ in (34) and combining the result of Proposition 2 yields the result of Proposition 3.

Therefore, the suboptimality in the asynchronous subgradient over the synchronous version is bounded by a constant proportional to $D_{\max}$. Note that if the dual method would like to reach a given distance from the optimal, the

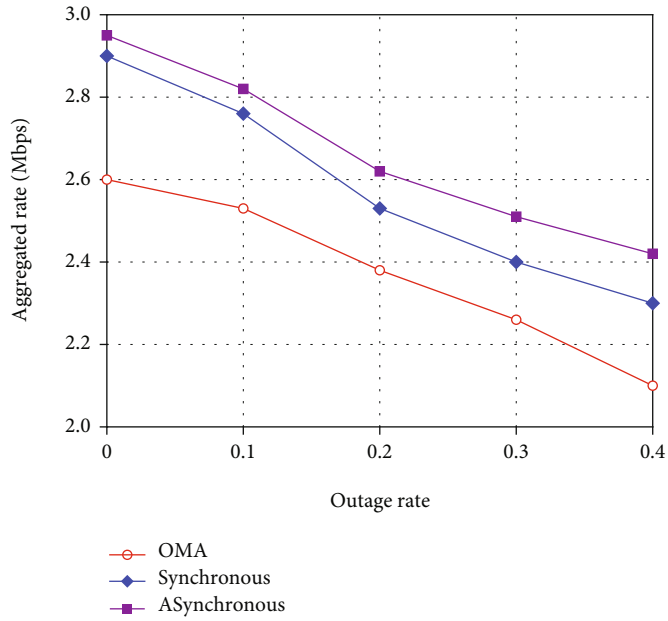

Figure 10: The aggregated rate under different outage rates, where each subchannel is assigned two UAVs.

asynchronous subgradient might need a smaller stepsize β which requires more iterations.

5. Simulation Results

In this paper, we use OMNET++5.0 to simulate the network scenario and collect relevant results. The UAVs spread randomly and uniformly in an area of 1000 m × 1000 m × 80 m and move following a random way-point mobility model [36]. In addition, we use the Rican channel model and rate threshold method to estimate the link quality. For convenience, we assume that there is only one GB with fixed coordinate, and UAVs can move randomly with a certain speed in the specified region. Each UAV transmits messages with different power levels in $(0, 1W]$, and final decisions can be made by solving the problem (19). The value of three stepsizes are set to 0.01 and $\Delta t = 1$ s. The detailed values of other parameters refer to the definitions in reference [37] and displayed in Table 1. To get more accurate results, we perform the experiment five times for each parameter under the same system configuration, and the final results are collected by computing the mean values based on the five groups of results.

To better demonstrate the advantages of the proposed method, we first analyze the performance of our algorithm and then compare it with OMA and synchronization optimization mechanism under different indicators. Because the wireless network is prone to be interfered by other signals, the outage rate is used as an important index to evaluate the performance of our algorithm. If each channel is assigned to two UAVs, the iterations increase with the outage rate, as shown in Figure 2. When UAVs send messages to GB over the unreliable uplink, some messages cannot be received by GB, which requires more iterations at GB to achieve the optimal network performance. When the outage rate is set to 0, Figure 3 shows the trends of the transmission rates of two UAVs in the same channel and their aggregated rate with the increase of iterations.

One of the main advantages of NOMA is that it allows multiple users to send messages on the same channel simultaneously. GB uses successive interference cancellation technique to decode superimposed signals. However, with the increasing number of nodes, the probability of GB that correctly receives all the messages decreases with the probability theory; hence, more iterations are required at GB to achieve the optimization goal, as shown in Figure 4. From Figure 5 we can see, the aggregated rate of single subchannel with more UAVs is larger; however, the existence of outage rate results in the decline of aggregated rate. The rate threshold characterizes the minimum transmission rate used by each UAV that GB can correctly decode the superimposed signals. Figure 6 represents the trend of aggregated rate with different rate thresholds, when there are four UAVs in a single channel. However, faster mobility will result in poor communication quality and decrease the aggregated rate of the single channel with two UAVs, as shown in Figure 7.

So far, we evaluate the performance of the proposed algorithm under different indicators, and the results are shown in Figures 2–7. However, we are more eager to know the performance of our algorithm compared with both OMA and synchronous method [19], and the details can be found in Figures 8 and 9. When the rate threshold is set to 0.5 Mbps, the UAVs move at a speed of 5 m/s, and the number of UAVs served each channel is no more than 2; from Figure 8, we can see that the aggregated rate of the single channel increases with the number of UAVs. The mobility of UAV leads to the variable channel state which brings unpredictable outage events, which declines the overall network performances. In order to reduce the impact of UAV mobility on communication quality, we use the expected

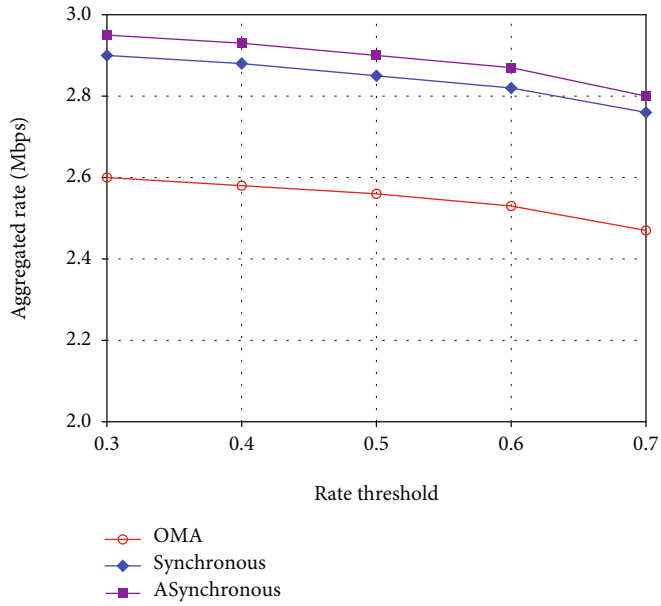

Figure 11: The aggregated rate under different rate thresholds, where each subchannel is assigned two UAVs.

channel gain to characterize the channel state in a specific time interval, which can be adapted to the dynamic channel well. Furthermore, the asynchronous optimization technique is used to optimize the network performance, and when some messages cannot be decoded correctly by GB, the algorithm will continue. OMA technique requires that each channel can only serve one single UAV at a specific instant, and the aggregated rate in our simulation is the throughput per second of the single channel. Hence, as the number of UAVs increases, the aggregated rate of the single channel maintains unchanged. Based on this, it is obvious that our algorithm has better performance than OMA and synchronous method as shown in Figures 8 and 9.

The interference prone property of the wireless channel increases the outage rate of multi-UAV networks, which would decrease the size of the aggregated rate of each channel. Different from synchronous methods, the asynchronous method updates the network parameters with the outdated channel gains of UAVs, where the outdated messages refer to the parameters used in previous iteration but the new ones have not yet received by GB in current iterations due to the poor channel states. Therefore, the presence of outage rate results in the decline of aggregated rate as shown in Figure 10. The rate threshold characterizes the minimum transmission rate used by each UAV that GB can correctly decode the superimposed signals. The increasing of the rate threshold requires the higher power levels to ensure the correct decoding at GB, the growth trend of the rate threshold would cause the channel capacity calculated with the optimal power level not to meet the constraint, and the detailed results are displayed in Figure 11.

6. Conclusion

This work presents channel allocation and power control algorithms for uplink NOMA-assisted multi-UAV networks by jointly using the Lagrange dual method, successive convex approximation, and asynchronous optimization method, which can improve network throughput, and reduce cochannel interference. Specifically, the original optimization problem is formulated as a mixed integer nonlinear programming framework. According to the differences between channel gain with nondescending order, each UAV is assigned to one specific channel. Combining the solution of channel allocation and adjusted initial power levels, the transmission power of UAVs is optimized with asynchronous update mechanism. Simulation results demonstrate that the proposed algorithm significantly improves aggregated rate about 5%-10% on average compared with similar works and OMA. Note that some open issues still exist, such as the security problem and QoS-aware (such as link reliability, delay bound) communication problem. In the future, more effort will be made to consider these problems and relevant techniques in optimization strategy.

Notations

W: Bandwidth
K: The maximum number of UAVs served by each channel
C: A set including all channels
c_n: An identifier of n-th channel
$|C|$: The total number of the channels
M: A set composed of all UAVs
M: The total number of UAVs in the network
M_n: The set of UAVs assigned to channel c_n
p_m: The power level used by UAVm to transmit message
$p_{\min}$: Minimum power level
$p_{\max}$: Maximum power level
y: The distance between UAV and GB
$\bar{h}$: Average channel gain
The variance of additive white Gaussian noise

σ^2:

g_m: The normalized channel gain of mth UAV.

Data Availability

The data that support the findings of this study are available from the corresponding author upon reasonable request.

Conflicts of Interest

The authors declare that there are no conflicts of interest concerning the publication of this paper.

Acknowledgments

This work is supported by China Postdoctoral Science Foundation (No. 2020M683156), Guangdong-Macau Joint Laboratory for Advanced and Intelligent Computing (No. 2020B1212030003), and Guangdong-Macau Joint STI Project Intelligent Target Detecting and Tracking on Electronic Fence of Funder Grant Number (No. 2021A0505080008).

References

[1] N. Mohamed, J. al-Jaroodi, I. Jawhar, A. Idries, and F. Mohammed, "Unmanned aerial vehicles applications in future smart cities," *Technological Forecasting and Social Change*, vol. 153, article 119293, 2020.

[2] Y. Zeng, J. Lyu, and R. Zhang, "Cellular-connected UAV: potential, challenges and promising technologies," *IEEE Wireless Communications*, vol. 26, no. 1, pp. 120–127, 2019.

[3] D. Liu, L. Wang, Y. Chen et al., "User association in 5G networks: a survey and an outlook," *IEEE Communications Surveys & Tutorials*, vol. 18, no. 2, pp. 1018–1044, 2016.

[4] M. Liaqat, K. A. Noordin, T. Abdul Latef, and K. Dimyati, "Power-domain non orthogonal multiple access (PD-NOMA) in cooperative networks: an overview," *Wireless Networks*, vol. 26, no. 1, pp. 181–203, 2020.

[5] K. W. Guvenc, I. Matolak, D. W. Fiebig, and S. N. Uwe-Carsten, "A survey of air-to-ground propagation channel modeling for unmanned aerial vehicles," *IEEE Communications Surveys & Tutorials*, vol. 21, no. 3, pp. 2361–2391, 2019.

[6] Y. Shen, X. Huang, B. Yang, and S. Wang, "Low complexity resource allocation algorithms for chunk based OFDMA multi-user networks with max-min fairness," *Computer Communications*, vol. 163, pp. 51–64, 2020.

[7] Z. Sun, Y. Jing, and X. Yu, "NOMA design with power-outage tradeoff for two-user systems," *IEEE Wireless Communications Letter*, vol. 9, no. 8, pp. 1278–1282, 2020.

[8] S. Wen and C. Huang, "Asynchronous distributed optimization via dual decomposition for delay- constrained flying ad hoc networks," *Computer Communications*, vol. 137, pp. 70–80, 2019.

[9] A. Kumar, K. Kumar, M. S. Gupta, and S. Kumar, "A survey on NOMA techniques for 5G scenario," in *Proceedings of the International Conference on Advances in Electronics, Electrical & Computational Intelligence (ICAEEC) 2019*, pp. 1–13, Allahabad India, 2019.

[10] M. Vaezi, G. A. A. Baduge, Y. Liu, A. Arafa, F. Fang, and Z. Ding, "Interplay between NOMA and other emerging technologies: a survey," *IEEE Transactions on Cognitive Communications and Networking*, vol. 5, no. 4, pp. 3104–3117, 2019.

[11] M. Pischella, I. Stupia, and L. Vandendorpe, "Performance analysis of uplink adaptive NOMA Depending on Channel Knowledge," 2020, https://arxiv.org/abs/2004.02630.

[12] E. Iradier, J. Montalban, L. Fanari et al., "Using NOMA for enabling broadcast/unicast convergence in 5G networks," *IEEE Transactions on Broadcasting*, vol. 66, no. 2, pp. 503–514, 2020.

[13] T. Z. H. Ernest, A. S. Madhukumar, R. P. Sirigina, and A. K. Krishna, "NOMA-aided multi-UAV communications in full-duplex heterogeneous networks,," *IEEE Systems Journal*, vol. 15, no. 2, pp. 2755–2766, 2021.

[14] Y. Liang, X. Li, and M. Haenggi, "Non-orthogonal multiple access (NOMA) in uplink Poisson cellular networks with power control," *IEEE Transactions on Communications*, vol. 67, no. 11, pp. 8021–8036, 2019.

[15] M. Zeng, A. Yadav, O. A. Dobre, and H. V. Poor, "Energy-efficient joint user-RB association and power allocation for uplink hybrid NOMA-OMA," *IEEE Internet of Things Journal*, vol. 6, no. 3, pp. 5119–5131, 2019.

[16] Y.-H. Chen, Y.-F. Chen, S.-M. Tseng, and D.-F. Tseng, "Low complexity user selection and power allocation for uplink NOMA beamforming systems," *Wireless Personal Communications*, vol. 111, no. 3, pp. 1413–1429, 2020.

[17] G. Zhao, Y. Li, C. Xu, Z. Han, Y. Xing, and S. Yu, "Joint power control and channel allocation for interference mitigation based on reinforcement learning," *IEEE Access*, vol. 7, pp. 177254–177265, 2019.

[18] B. Rashid, A. Ahmad, S. Saleem, and A. Khan, "Joint energy efficient power and subchannel allocation for uplink MC-NOMA networks," *International Journal of Communication Systems*, vol. 4606, pp. 1–18, 2020.

[19] J. Zhang, L. Zhu, Z. Xiao, X. Cao, D. O. Wu, and X.-G. Xia, "Optimal and sub-optimal uplink NOMA: joint user grouping, decoding order, and power control," *IEEE Wireless Communications Letters*, vol. 9, no. 2, pp. 254–257, 2020.

[20] M. R. Zamani, M. Eslami, M. Khorramizadeh, H. Zamani, and Z. Ding, "Optimizing weighted-sum energy efficiency in downlink and uplink NOMA systems," *IEEE Transactions on Vehicular Technology*, vol. 69, no. 10, pp. 11112–11127, 2020.

[21] J. Lu, Y. Wang, T. Liu et al., "UAV-enabled uplink non-orthogonal multiple access system: joint deployment and power control," *IEEE Transactions on Vehicular Technology*, vol. 69, no. 9, pp. 10090–10102, 2020.

[22] X. Chen, D. Li, Z. Yang et al., "Securing aerial-ground transmission for NOMA-UAV networks," *IEEE Network*, vol. 34, no. 6, pp. 171–177, 2020.

[23] R. Tang, J. Cheng, and Z. Cao, "Joint placement design, admission control, and power allocation for NOMA-based UAV systems," *IEEE Wireless Communications Letters*, vol. 9, no. 3, pp. 385–388, 2020.

[24] S. Zhang, Y. Zeng, and R. Zhang, "Cellular-enabled UAV communication: a connectivity constrained trajectory optimization perspective," *IEEE Transactions on Communications*, vol. 67, no. 3, pp. 2580–2604, 2019.

[25] N. Senadhira, S. Durrani, X. Zhou, N. Yang, and M. Ding, "Uplink NOMA for cellular-connected UAV: impact of UAV trajectories and altitude," *IEEE Transactions on Communications*, vol. 68, no. 8, pp. 5242–5258, 2020.

[26] X. Pang, G. Gui, N. Zhao et al., "Uplink precoding optimization for NOMA cellular-connected UAV networks," *IEEE Transactions on Communications*, vol. 68, no. 2, pp. 1271–1283, 2020.

[27] W. K. New, C. Y. Leow, K. Navaie, and Z. Ding, "Robust non-orthogonal multiple access for aerial and ground users," *IEEE Transactions on Wireless Communications*, vol. 19, no. 7, pp. 4793–4805, 2020.

[28] M. Grau Novellas, R. Serra, and M. Rose, "Methodology for coupling and interference prediction in integrated-circuit substrates," *IEEE Transactions on Electromagnetic Compatibility*, vol. 58, no. 4, pp. 1118–1127, 2016.

[29] Y. R. Cong, X. Y. Zhou, and R. A. Kennedy, "Interference prediction in mobile ad hoc networks with a general mobility model," *IEEE Transactions on Wireless Communication*, vol. 14, no. 8, pp. 4277–4290, 2015.

[30] M. Kim and J. Lee, "Outage probability of UAV communications in the presence of interference," in *2018 IEEE Global Communications Conference (GLOBECOM)*, pp. 1–6, Abu Dhabi, United Arab Emirates, 2018.

[31] S. Yan, X. R. Zhang, H. Y. Xiang, and W. Wu, "Joint access mode selection and Spectrum allocation for fog computing based vehicular networks," *IEEE Access*, vol. 7, pp. 17725–17735, 2019.

[32] M. S. Ali, H. Tabassum, and E. Hossain, "Dynamic user clustering and power allocation for uplink and downlink non-orthogonal multiple access (NOMA) systems," *IEEE Access*, vol. 4, pp. 6325–6343, 2016.

[33] J. Papandriopoulos and J. S. Evans, "SCALE: a low-complexity distributed protocol for spectrum balancing in multiuser DSL networks," *IEEE Transactions on Information Theory*, vol. 55, no. 8, pp. 3711–3724, 2009.

[34] M. Sinaie, D. W. K. Ng, and E. A. Jorswieck, "Resource allocation in noma virtualized wireless networks under statistical delay constraints," *IEEE Wireless Communications Letters*, vol. 7, no. 6, pp. 954–957, 2018.

[35] K. Rajawat, N. Gatsis, and G. B. Giannakis, "Cross-layer designs in coded wireless fading networks with multicast," *IEEE/ACM Trans. Netw.*, vol. 19, no. 5, pp. 1276–1289, 2011.

[36] K. Peters, A. E. K. Çetinkaya, and J. P. G. Sterbenz, "A geographical routing protocol for highly-dynamic aeronautical networks," in *2011 IEEE Wireless Communications and Networking Conference*, pp. 492–497, Cancun, Mexico, 2011.

[37] D. W. Matolak and R. Sun, "Air-ground channel characterization for unmanned aircraft systems-part I: methods, measurements, and models for over-water settings," *IEEE Transactions on Vehicular Technology*, vol. 66, no. 1, pp. 26–44, 2017.